On page 38, please amend Table 1 to read:

Table 1.

SEQ ID NO:	1	2	3	4	5	6	7	8	9	10	11
Predicted Hairpin Secondary Structure	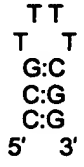	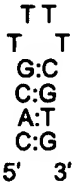				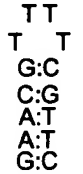	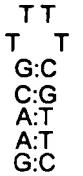	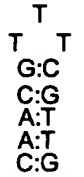	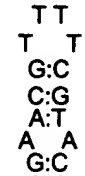	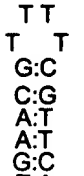	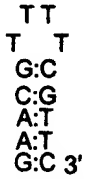
Identity	3bp	4bp	5bp	6bp	7bp	8bp	9bp	5bp3dT	6bpA$_{14}$	7bp5'dT	Dumb-bell
ΔG [b] (Kcal/mol)	-3.0	-4.5	-5.6	-8.2	-9.0	-11.4	-12.8	-4.2	-4.3	-9.8	-11.3
I/Io [c] (%)	68	64	60	52	47	35	32	62	53	45	NA
Blockade Duration (median in ms)	0.8	5	68	760	3200	NA	NA	21	5	3700	NA

On page 43, please amend the paragraph starting on line 17 to read:

Figure 3c shows blockade patterns where only the terminal base pair differed between molecules. Thus, individual DNA molecules with terminal G-C (SEQ ID NO:17), A-T (SEQ ID NO:19), and G-T (SEQ ID NO:20) base pairs could be distinguished from one-another.

On page 43, please amend the paragraph starting on line 22 to read:

We found that single nucleotide alterations in DNA could be detected using the nanopore instrument. Here we present two examples. The first example involved the hairpin loop. A 5bp hairpin with a 3-deoxythymidine loop (5bp3dT in Table 1; SEQ ID NO:8) caused pore blockades in

which the shoulder amplitude was increased ≅2 pA and the median shoulder duration (21 ms) was reduced 3-fold relative to the same hairpin stem with a 4-deoxythymidine loop (5bp in Table 1; SEQ ID NO:3). Typical events are illustrated in Figure 4a. The FSA acquired 3500 possible 5 bp hairpin signals from ten minutes of recorded data. The SVM classification for this data set (Figure 4b) gave sensitivity and specificity values of 99.9% when 788 events were rejected as the unknown class. The second example involved the hairpin stem. Introduction of a single base-pair mismatch into the stem of a 6-bp hairpin ($T_{14}\rightarrow A_{14}$, $6bpA_{14}$ in Table 1; SEQ ID NO:9) caused approximately a 100-fold decrease in the median blockade shoulder duration relative to a hairpin with a perfectly matched stem (6bp in Table 1; SEQ ID NO:4). Typical events are shown in Figure 4c. This difference in duration is consistent with the effect of a mismatch on ΔG° of hairpin formation (Figure 2), and it permitted a 90% separation of the two populations using the manually applied shoulder-spike diagnostic. When analysis was automated, the FSA acquired 1031 possible events from ten minutes of recorded data (Figure 4d). With the aid of wavelet features (Nievergelt, Y. Wavelets Made Easy. (Birkhauser, Boston; 1999)) that characterize the low frequency noise within the shoulder current, the SVM was able to discriminate the standard 6 bp hairpin (SEQ ID NO:4) from the mismatched $6bpA_{14}$ hairpin (SEQ ID NO:9) with sensitivity 97.6% and specificity 99.9% while rejecting only 42 events.

a4 cont

On page 44, please amend the paragraph starting on line 19 to read:

For longer hairpin stems (or for native duplex DNA), very long shoulder blockades preclude rapid identification of each captured molecule. For example, the shoulder duration for a hairpin with as few as 8 base pairs ranged up to 300 seconds resulting in a very small number of measurable events in a 30-minute experiment (Figure 3a). To overcome this limitation, we modified the acquisition protocol from a fixed +120 mV potential to a voltage pulse routine that toggled between +120 mV for 249.5 ms and -40 mV for 0.1 ms. In essence, the routine was designed to capture and examine each hairpin stem for a finite amount of time under standard conditions then eject the hairpin rather than pulling it through the pore. Representative blockades for 7 bp (SEQ ID NO:5), 8 bp (SEQ ID NO:6), and 9 bp (SEQ ID NO:7) stems using this acquisition protocol are shown in Figure 5. Shoulder blockades caused by the 8bp and 9bp hairpins toggled between two conductance states. The greater of these states corresponded to the average conductance for the 7bp hairpin. The

a5

lesser conductance states for the 8bp and 9bp hairpins were nearly equal with one another, however transitions between the two states were significantly more frequent for the 8bp hairpin than for the 9bp hairpin. We postulate that these two conductance states represent transient interaction of the terminal base pair of the 8 bp and 9 bp hairpins with amino residues in the vestibule wall near the limiting aperture. This explanation predicts that single nucleotide or single base pair modifications at the end of the 8 and 9 bp hairpin stems would alter the rate of transition between conductance states.

a5

On page 45, please amend the paragraph starting on line 17 to read:

The nanopore device can also be used to discriminate among the four permutations of Watson-Crick base pairs at 9bp DNA hairpin termini. The DNA hairpins we used are shown in Table 2 and are abbreviated as 9bp(CT/GA; SEQ ID NO:13), 9bp(GT/CA; SEQ ID NO:12), 9bp(TT/AA; SEQ ID NO:15), and 9bp(AT/TA; SEQ ID NO:14) where the two letters before the slash are the first two bases in the hairpin sequence reading from 5′-to-3′, and the two letters after the slash are the last two bases in the hairpin sequence reading from 3′-to-5′. Table 2 appears in Figure 8. Examples of thousands of pore blockades for each of these hairpins are shown in Figure 9. Terminal base-pair identity can be determined by kinetic analysis of the nanopore data. In particular, average dwell time in the lower conductance level (LL in Figure 10) and the frequency of downward current spikes (S in Figure 10) are highly dependent upon the presence of a base pair in the ninth position. This is illustrated in Figure 11 where neither a 5′ dC dangling nucleotide nor a 3′ dG dangling nucleotide alone stabilized ionic current in the lower level (I/Io = 32%), whereas both nucleotides together (the CG pair) did so. It was conceivable that the presence of two nucleotides alone at the terminus of the hairpin stem could account for this current stabilization. However, two weakly paired thymine bases at the blunt end terminus of a 9bp hairpin stem resulted in an unstable blockade signature (Figure 11). In practice, the lower conductance level has the added advantage that transitions to UL are stochastic, and that one first order exponential can be fit to the dwell time distribution giving a time constant (τ_{LL}) in the millisecond range.

a6

On page 46, please amend the paragraph starting on line 8 to read:

To test the sensitivity of the lower level conductance state to Watson-Crick base-pair identity, we measured τ_{LL} and spike frequency for the four 9 bp hairpins whose blockade signatures are illustrated in Figure 9. Dwell time histograms for the lower conductance state caused by 9bp(GT/CA; SEQ ID NO:12) and by 9bp(TT/AA; SEQ ID NO:15) are shown in Figure 12. First-order exponentials fit to similar histograms for all four permutations of Watson-Crick base-pairs reveal τ_{LL} values ranging from 160 ms to 7 ms in the order 9bp(GT/CA; SEQ ID NO:12) > 9bp(CT/GA; SEQ ID NO:13) > 9bp(AT/TA; SEQ ID NO:14) > 9bp(TT/AA; SEQ ID NO:15) (Table 3).

On page 46, please amend Table 3 starting on line 24 to read:

Identity	τ_{LL} ms	Spike frequency s^{-1}	$\Delta\Delta G°_{term}$ kcal/mol
9bpGT/CA (SEQ ID NO:12)	160 ± 23	4 ± 1	-1.9
9bpCT/GA (SEQ ID NO:13)	50 ± 4	12 ± 4	-1.8
9bpAT/TA (SEQ ID NO:14)	43 ± 5	34 ± 10	-1.2
9bpTT/AA (SEQ ID NO:15)	7 ± 1	91 ± 47	-1.3
9bpTT/GA (SEQ ID NO:16)	6 ± 2	1300 ± 400	-0.3

On page 47, please amend the paragraph starting at line 1 to read:

The reverse order is observed for the spike frequency ranging from 4 spikes s^{-1} (9bp(GT/CA; SEQ ID NO.12)) to 82 spikes s^{-1} (9bp(TT/AA; SEQ ID NO.15)). Thus, two easily measured kinetic parameters can be used to discriminate among Watson-Crick base pairs on single DNA molecules.

On page 47, please amend the paragraph starting at line 5 to read:

One of the more difficult base-pairs to recognize using conventional hybridization arrays is a terminal mismatch, in particular a TG wobble pair. To test the sensitivity of the nanopore to this mismatch, we compared blockade signatures caused by a hairpin composed of the sequence 9bp(TT/GA; SEQ ID NO.16) with blockade signatures caused by the wild-type sequences

9bp(CT/GA; SEQ ID NO.13) and 9bp(TT/AA; SEQ ID NO.15) (Figure 9). All individual blockades that exhibited the characteristic four current level signature could be identified as one of these molecules. Quantitative examination of the data revealed that spike frequency was the key diagnostic parameter. That is, there was a statistically significant difference between spike frequencies caused by each of the three termini, i.e. 12 spikes s^{-1} (9bp(CT/GA; SEQ ID NO.13)), 82 spikes s^{-1} (9bp(TT/AA; SEQ ID NO.15)), and 1400 spikes s^{-1} (9bp(TT/GA; SEQ ID NO.16)) (Table 2). In contrast, τ_{LL} values were statistically different between 9bp(TT/GA; SEQ ID NO.16) and 9bp(CT/GA; SEQ ID NO.13) termini, but not between 9bp(TT/G6; SEQ ID NO.15) and (9bp(TT/AA; SEQ ID NO.15) termini (Table 3). It appears that τ_{LL} values plateau in the low millisecond time-range for any blunt-ended DNA terminus regardless of base-pair stability.

a9

On page 47, please amend the paragraph starting at line 19 to read:

The rankings of spike frequency and τ_{LL} correlate with conventional estimates of terminal base-pair stability. Table 3 lists free energy values for terminal base pairs ($\Delta\Delta G°_{Term}$) calculated using the online computational tool 'Mfold' (http://bioinfo.math.rpi.edu/~mfold/dna/form1.cgi) which is based on a nearest neighbor model of duplex stability. In Table 3, the $\Delta\Delta G°_{Term}$ values are the difference between the free energy of duplex formation for a given 9bp hairpin and the free energy of duplex formation of a common 8bp core hairpin sequence. Among Watson-Crick base pairs, $\Delta\Delta G°_{Term}$ values ranged from –1.9 kcal/mol for 9bp(GT/CA; SEQ ID NO:12) to –1.2 kcal/mol for 9bp(AT/TA; SEQ ID NO:14). $\Delta\Delta G°_{Term}$ for the TG wobble pair was calculated to be –0.3 kcal/mol. In general, the rank of spike frequency and τ_{LL} correlated with $\Delta\Delta G°_{Term}$, however the correlation is imperfect in that the expected order of 9bp(TT/AA; SEQ ID NO:15) and 9bp(AT/TA; SEQ ID NO:14) was reversed. There are several possible explanations for this discrepancy including uncertainty surrounding the predicted stability of terminal 5′-A•T-3′ and 5′-T•A-3′ pairs[2,7], and limits on the precision of optical melting curves that underlie the free energy calculations. We note that the calculated $\Delta\Delta G°_{Term}$ values for the 9bp(AT/TA; SEQ ID NO:14) and 9bp(TT/AA; SEQ ID NO:15) termini differed by only 0.1 kcal/mol (Table 3) which is smaller than the 5% precision given for Mfold. It is also important to note that base-pair stability is influenced by the electric field (data not shown) and possibly by amino acids in the vestibule wall. The magnitude

a10

a10 of these effects could be sequence dependent, thus altering the stability ranking in the nanopore assay relative to a bulk solution assay.

On page 48, please amend the paragraph starting at line 19 to read:

Initial inspection of the data in Table 3 suggests that hydrogen bonding plays a significant role in spike frequency and τ_{LL}. That is, terminal base pairs that are known to form three hydrogen bonds when paired (GC and CG) are more stable than base-pairs that are known to form two hydrogen bonds when paired (AT, TA, and TG). However, in practice it is difficult to assign a stability change to hydrogen bonding alone. This is illustrated by comparing the TG wobble pair and the CG Watson-Crick base-pair. In substituting a 5′ thymidine for a 5′ cytosine at the 9bp hairpin terminus, hydrogen bond number is reduced from three to two, but stacking energy is stabilized by –0.1 kcal/mol as shown by melting curves for DNA duplexes with dangling ends. Although small, this change in stacking energy is comparable to calculated differences in $\Delta\Delta G°_{Term}$ between some of the terminal base-pairs in Table 3. Thus, the change in blockade signature associated with the CG→TG terminal substitution is due to the combined effect of added stacking stabilization by thymine and destabilization by loss of hydrogen bonds. Competing effects are also likely when the thymine in the terminal TA base-pair is replaced by difluorotoluene (9bpTT/AA→9bpFT/AA; SEQ ID NO:18). Difluorotoluene is a near perfect structural mimic of thymine that is recognized nearly as well by DNA polymerases despite the absence of hydrogen bonding to paired adenines. This isostere would be an ideal tool to assess the influence of hydrogen bonding on τ_{LL} and spike frequency, however, difluorotoluene is nonpolar and its stacking interaction with neighboring bases stabilizes the duplex by –1.5 kcal/mol relative to thymine. Thus, the blockade signature due to 9bpTT/AA→9bpFT/AA (SEQ ID NO:18) (Figure 13) is a conservative measure of destabilization due to loss of hydrogen bonding because it is partially offset by added stacking stability.

a11

On page 49, please amend the paragraph starting at line 13 to read:

a12 The data in Table 3 also indicate that orientation of the bases in the terminal pair influences spike frequency and τ_{LL}. That is, flipping the terminal base-pair so that a purine is on the 5′ side and

a pyrimidine is on the 3′ side (9bp(CT/GA; SEQ ID NO:13)→9bp(GT/CA; SEQ ID NO:12) and 9bp(TT/AA; SEQ ID NO:15)→9bp(AT/TA; SEQ ID NO:14)) consistently increased τ_{LL} and decreased spike frequency. Among Watson-Crick base-pairs, the size of this effect equals or exceeds the effect of increasing hydrogen bond number (Table 3). Classical thermodynamic studies suggest two possible explanations: i) stacking forces with the neighboring base-pair are altered when the terminal base-pair is flipped; and ii) stacking of bases at the 5′ position of a duplex can be different from those at the 3′ position independent of the neighboring base-pair. To test the first explanation, we compared τ_{LL} for the standard 9bp hairpins containing the four possible Watson-Crick termini (Table 2 at left) with their counterparts in which the penultimate TA base-pair was flipped, i.e. hairpins 9bp(TA/AT; SEQ ID NO:22), 9bp(AA/TT; SEQ ID NO:21), 9bp(CA/GT; SEQ ID NO:20) and 9bp(GA/CT; SEQ ID NO:19) at right in Table 2. 9bp(TT/AA; SEQ ID NO:15) was the least stable of the original sequences with τ_{LL} equal to 7 ms. By making the substitution 9bp(TT/AA; SEQ ID NO:15)→ 9bp(TA/AT; SEQ ID NO:22), τ_{LL} was increased about three-fold to 20 ms (Table 4).

a12

On page 50, please amend the paragraph starting at line 9 to read:

Conversely, 9bp(AT/TA; SEQ ID NO:14) was the most stable of the thymidine/adenine termini with τ_{LL} equal to 43 ms. By making the same alteration of the neighboring base-pair as in the previous experiment, 9bp(AT/TA; SEQ ID NO:14)→9bp(AA/TT; SEQ ID NO:21), τ_{LL} was decreased to 30 ms. Thus, stacking against the neighboring base-pair did account for much of the stability difference associated with orientation of the thymine/adenine termini. The independent effect of placing adenine at the 5′ position was small. For the guanine/cytosine termini, the outcome was very different (Table 3). In those cases, flipping penultimate base pairs did not significantly effect τ_{LL}. Thus, the three-fold difference in τ_{LL} for 5′-G•C-3′ versus 5′-C•G-3′ is due to an end-specific effect independent of the neighboring base-pair.

a13

I. REMARKS

Formal Matters

Claims 1-20 are pending after entry of the amendments set forth herein.